Enhanced adaptive matched filter for automated identification and measurement of electrocardiographic alternans

Marcantoni, I.; Sbrollini, A.; Morettini, M.; Swenne, C.A.; Burattini, L.

Biomedical Signal Processing and Control 68 (2021) 102619

Contents lists available at ScienceDirect

Biomedical Signal Processing and Control

journal homepage: www.elsevier.com/locate/bspc

Enhanced adaptive matched filter for automated identification and measurement of electrocardiographic alternans

Ilaria Marcantoni [a], Agnese Sbrollini [a], Micaela Morettini [a], Cees A. Swenne [b], Laura Burattini [a,*]

[a] Department of Information Engineering, Università Politecnica delle Marche, Ancona, Italy
[b] Cardiology Department, Leiden University Medical Center, Leiden, the Netherlands

ARTICLE INFO

Keywords:
Heart electrical instability
Cardiac risk index
Digital electrocardiogram processing
P-wave alternans
QRS-complex alternans
T-wave alternans

ABSTRACT

Electrocardiographic alternans, consisting of P-wave alternans (PWA), QRS-complex alternans (QRSA) and T-wave alternans (TWA), is an index of cardiac risk. However, only automated TWA measurement methods have been proposed so far. Here, we presented the enhanced adaptive matched filter (EAMF) method and tested its reliability in both simulated and experimental conditions. Our methodological novelty consists in the introduction of a signal enhancement procedure according to which all sections of the electrocardiogram (ECG) but the wave of interest are set to baseline, and in the extraction of the alternans area (AAr) in addition to the standard alternans amplitude (AAm). Simulated data consisted of 27 simulated ECGs representing all combinations of PWA, QRSA and TWA of low (10 μV) and high (100 μV) amplitude. Experimental data consisted of exercise 12-lead ECGs from 266 heart failure patients with an implanted cardioverter defibrillator for primary prevention. EAMF was able to accurately identify and measure all kinds of simulated alternans (absolute maximum error equal to 2%). Moreover, different alternans kinds were simultaneously present in the experimental data and EAMF was able to identify and measure all of them (AAr: 545 μV × ms, 762 μV × ms and 1382 μV × ms; AAm: 5 μV, 9 μV and 7 μV; for PWA, QRSA and TWA, respectively) and to discriminate TWA as the prevalent one (with the highest AAr). EAMF accurately identifies and measures all kinds of electrocardiographic alternans. EAMF may support determination of incremental clinical utility of PWA and QRSA with respect to TWA only.

1. Introduction

Heterogeneity in cardiac tissue is fundamental to maintain the normal electrical and mechanical heart function [1]. However, pathological conditions and administration of drugs may lead to an exacerbation of such heterogeneities that, in turn, may result in an increased risk of cardiac arrhythmias [1]. Indeed, the occurrence of dynamic factors, interacting with each other and/or with pre-existing tissue heterogeneities, may cause arrhythmogenic cardiac alternans [1]. At the cellular level, cardiac alternans manifests as every-other-beat alternation in contraction (mechanical alternans), action potential duration (electrical alternans) and cytosolic calcium transient amplitude [2]. Indeed, in myocytes the beat-to-beat regulation of cytosolic calcium is linked to membrane potential and it is generally agreed that this link is a key factor causing electromechanical and calcium transient alternans [2]. Electromechanical and calcium transient alternans are highly correlated, but it has remained moot whether the primary cause of the phenomenon is a perturbation of cytosolic calcium signaling or membrane electrical properties [2]. This coupling was studied in case of ventricular myocytes but less in case of atrial ones [2].

Given the cellular mechanism underlying the phenomenon, cardiac alternans manifests in the electrocardiogram (ECG). Electrocardiographic alternans (ECGA) is the manifestation of an electrophysiological phenomenon occurring at stable heart rhythm consisting in the every-

Abbreviations: AAm, alternans amplitude; AAr, alternans area; EAMF, enhanced adaptive matched filter; ECG, electrocardiogram; ECGA, electrocardiographic alternans; f_A, alternans frequency; ICD, implanted cardioverter defibrillator; iqr, interquartile range; J, J point; mRR, mean RR interval; NHB, number of heartbeats; NS, number of seconds; Pon, P-wave onset; PWA, P-wave alternans; Qon, Q-wave onset; QRSA, QRS-complex alternans; SF, sampling frequency; stdRR, RR standard deviation; Tend, T-wave end; TWA, T-wave alternans.

* Corresponding author at: Department of Information Engineering, Università Politecnica delle Marche, Via Brecce Bianche 12, 60131, Ancona, Italy.
E-mail addresses: i.marcantoni@pm.univpm.it (I. Marcantoni), a.sbrollini@pm.univpm.it (A. Sbrollini), m.morettini@univpm.it (M. Morettini), c.a.swenne@lumc.nl (C.A. Swenne), l.burattini@univpm.it (L. Burattini).

https://doi.org/10.1016/j.bspc.2021.102619
Received 14 December 2020; Received in revised form 1 March 2021; Accepted 4 April 2021
Available online 10 April 2021

other-beat alternation of the morphology of one or more electrocardiographic waves (P wave, QRS complex or T wave), expressing in amplitude, shape or polarity variation. ECGA is a non-stationary phenomenon, with varying amplitude and duration [3,4]. Historically, alternans that manifests as T-wave oscillation in the ECG, i.e. T-wave alternans (TWA), was the most investigated. TWA has become an electrocardiographic prognostic means for arrhythmia-risk stratification and regulation of antiarrhythmic therapy [2,5–13]. It has been observed in several conditions: electrolyte abnormalities, hypothermia, coronary artery disease, post-myocardial infarction, long QT and Brugada syndromes, vasospastic angina, dilated, hypertrophic, and Takotsubo cardiomyopathies, and heart failure [1,14–25]. P-wave alternans (PWA) and QRS-complex alternans (QRSA) have been less investigated and most studies in the literature, especially those related to PWA, are case reports [26–36]. PWA has been referred as a rare phenomenon predictor of atrial fibrillation [26]. P wave is associated to atrial depolarization; thus, it is plausible to associate PWA to atrial electrical instabilities. Similarly, being QRS complex associated to ventricular depolarization, QRSA appeared mostly to occur in case of supraventricular and ventricular tachycardias [31–36]. Therefore, in general, ECGA is recognized as a risk factor for cardiac arrhythmias (including severe ventricular arrhythmias and atrial fibrillation) and even for sudden cardiac death. Given its importance, recently, it was recognized that investigation of ECGA would deserve a complete vision on the electrical function of all myocytes (both atrial and ventricular) and on all cardiac cycle phases (both diastolic and systolic) [37–39]. Further studies are needed to permit a comparison of results, as well as statistical and epidemiological evaluations for the ECGA phenomenon interpretation. The preliminary requirement to perform these studies is a reliable automated method able to identify and measure ECGA in all its possible manifestations, i.e. PWA, QRSA or TWA. As far as we know, no specially designed algorithm for automated identification and measurement of ECGA has been presented in the literature (the several proposed methods refer only to TWA and studies on PWA and QRSA relied mostly on visual inspection).

Thus, the present study aimed to propose an enhanced version of the heart-rate adaptive matched filter method, originally introduced to study only TWA [40], and to test it in the reliable identification and measurement of PWA, QRSA and TWA in both simulated and experimental conditions.

2. Materials and methods

The algorithm proposed here, termed enhanced adaptive matched filter (EAMF), is meant to investigate all kinds of ECGA (i.e. PWA, QRSA and TWA) and represents an enhanced version of the heart-rate adaptive matched filter algorithm, originally introduced to study alternans affecting only the T wave [40]. The EAMF was designed to process an ECG tracing containing a number of heartbeats (NHB) equal or greater than 32. In case of ECG signals longer than NHB heartbeats, analysis is still possible. In case, overlapping and sliding ECG windows containing NHB heartbeats are recursively extracted until the whole length of the signal is reached. The elapsed number of seconds (NS) between two subsequent extractions has to be equal or greater than 1 s [41,42]. There are no restrictions in the sampling frequency (SF) of the ECG signal to be analyzed as long as SF is equal or greater than 200 Hz.

The EAMF-based procedure to automatically identify and measure ECGA is described below and consists of two subsequent steps, a preprocessing step (including filtering, ECG suitability assessment and signal enhancement) and an alternans identification and measurement step by EAMF (including signal filtering and extraction of alternans features). As the ECGA is probably a lead-dependent phenomenon (analogously to TWA [43]), the procedure is performed on each available lead. In the description of the procedure, the generic NHB-heartbeat long ECG window of the generic lead is referred to as ECG tracing.

The block diagram of the whole procedure for automated ECGA identification and measurement through the EAMF is depicted in Fig. 1.

2.1. Preprocessing

Preprocessing of the raw ECG tracing includes standard high-frequency noise removal (by application of a 6th-order bidirectional Butterworth filter with cut-off frequency at 35 Hz), R-peak detection (mandatory if annotations are not available), heartbeat segmentation (mandatory if annotations are not available) and removal of baseline (computed through cubic spline interpolation).

Additionally, replacement of artifacts and ectopic heartbeats is performed. A check on the possible presence of noisy or non-sinus heartbeats is carried out through a correlative approach. At first, each heartbeat is sectioned into three adjoint sections (Fig. 2): the P-wave

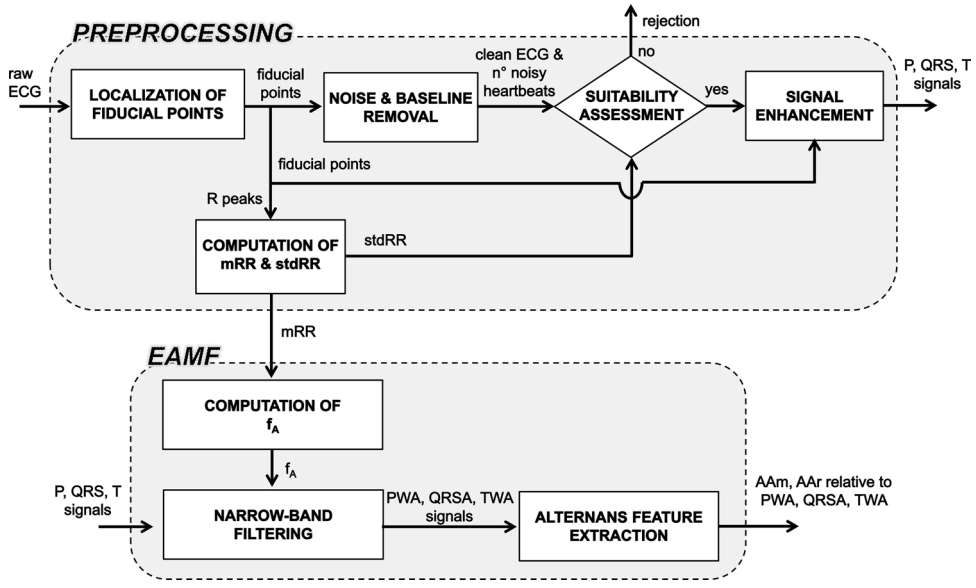

Fig. 1. Block diagram of the whole procedure for automated electrocardiographic alternans (ECGA) identification and measurement through the enhanced adaptive matched filter (EAMF).

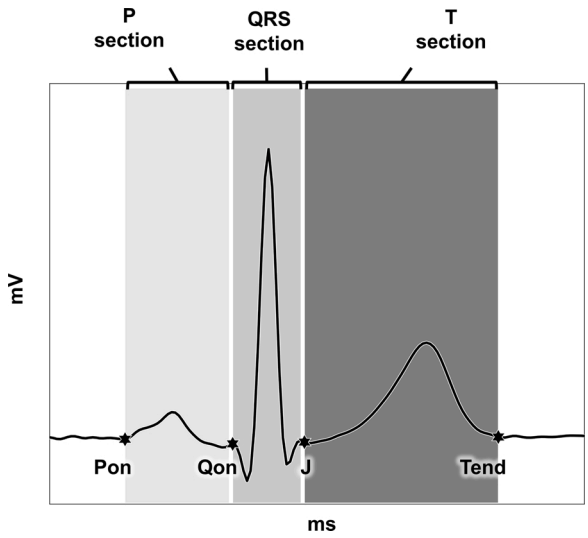

Fig. 2. The three adjoining sections inside a heartbeat: the P-wave section (P section), from the P-wave onset (Pon), to the Q-wave onset (Qon); the QRS-complex section (QRS section), from Qon, to the J point (J); and the T-wave section (T section), from J to the T-wave end (Tend). Different shades of gray discriminate adjacent sections; stars localize section landmarks.

section (P section), included between the P-wave onset (Pon) and the Q-wave onset (Qon); the QRS-complex section (QRS section), included between Qon and the J point (J); and the T-wave section (T section), included between J and the T-wave end (Tend).

If heartbeat landmarks are already annotated, they are used as landmarks of ECG sections; otherwise, they have to be estimated, for example through experimental formulas or through visual inspection. In the experimental study performed here, Pon was the only landmark that was not annotated, thus we estimated it experimentally (Pon = Qon – 160 ms).

Eventually, correlations between the ECG waveforms included in the QRS and T sections of each heartbeat and the corresponding ECG waveforms of the median heartbeat (computed over all available heartbeats) are evaluated. The heartbeat under examination is assumed to be sinus and not affected by artifacts if correlations relative to QRS and T waves are both higher than 0.85; if not, the heartbeat is entirely replaced by the median heartbeat. Moreover, R peaks are used to compute mean RR interval (mRR; s) and RR standard deviation (stdRR; s). An ECG tracing is considered suitable for ECGA analysis if its number of replaced heartbeats is lower than 10 % NHB and stdRR is less than 10 % mRR. If classified as not suitable, the ECG tracing is no further analyzed. Suitable ECG tracings undergo signal enhancement by setting to baseline all ECG sections but the one for which occurrence of alternans has to be evaluated. Thus, from each ECG tracing, three signals are generated (Fig. 3): the P signal (with all sections set to baseline but the P section); the QRS signal (with all sections set to baseline but the QRS section); and the T signal (with all sections set to baseline but the T section).

2.2. Enhanced adaptive matched filter

In the unlikely condition of fixed heart rate (i.e. null heart-rate variability), alternans would have one specific frequency, by definition equal to half heart rate. However, in the realistic condition of stable heart rate but affected by a finite, although limited, physiological variability, ECGA is characterized by a narrow frequency band around half mean heart rate. Thus, in order to extract the alternans signal, a band-pass filter is conceived. After computing the alternans frequency ($f_A = 1/2 \cdot$mRR; Hz), the band-pass filter is implemented as a 6^{th}-order bidirectional (to avoid phase delay) Butterworth filter with high-pass

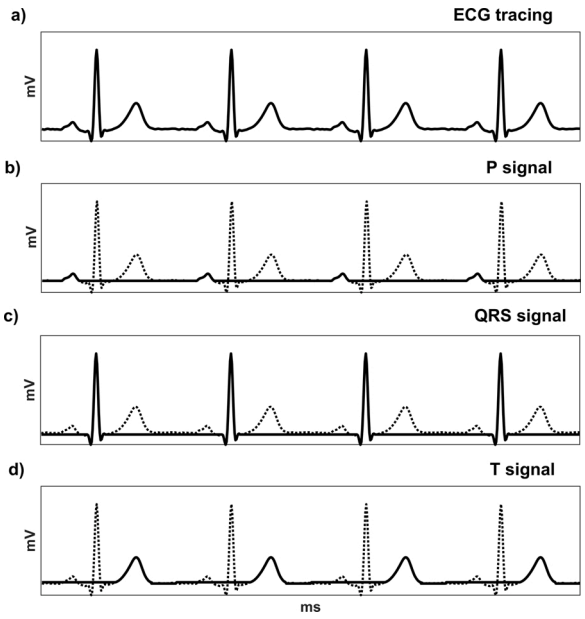

Fig. 3. Signal enhancement: from each electrocardiogram (ECG) tracing (panel a), three signals are generated by setting to baseline all ECG segments but the one for which occurrence of alternans has to be evaluated and are: the P signal (panel b), the QRS signal (panel c); and the T signal (panel d).

cut-off frequency of $f_L = f_A - 0.06$ Hz and low-pass cut-off frequency of $f_H = f_A + 0.06$ Hz [40]. The filter transfer function is given by (1):

$$|H(f)|^2 = |H_L(f)|^2 \cdot |H_H(f)|^2 = \frac{1}{1+\left(\frac{f}{f_L}\right)^6} \cdot \frac{\left(\frac{f}{f_H}\right)^6}{1+\left(\frac{f}{f_H}\right)^6} \quad (1)$$

When fed with a preprocessed signal (either P signal, QRS signal or T signal), this filter deletes any frequency component outside the alternans band and provides, as output, a pseudo-sinusoidal signal (Fig. 4). If the input signal is the P signal, the pseudo-sinusoid signal is termed PWA signal and has its maxima and minima in correspondence of the P wave;

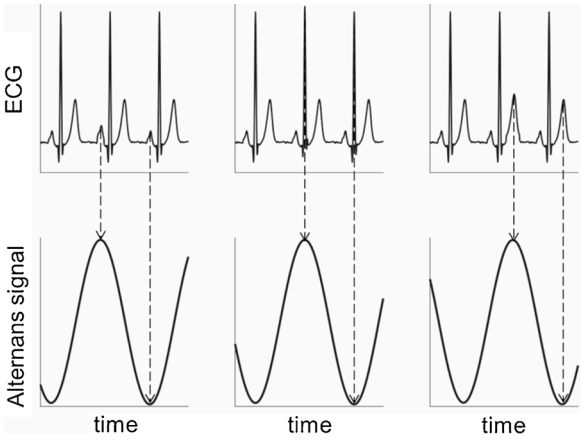

Fig. 4. Qualitative representation of the electrocardiogram (ECG, first row) and corresponding alternans signal (second row) at the output of the enhanced adaptive matched filter (EAMF) in case of P-wave alternans (PWA; first column), QRS-complex alternans (QRSA; second column) and T-wave alternans (TWA; third column). In all cases the alternans signal is a pseudo-sinusoid. However, the pseudo-sinusoid phase depends on the alternans kind: in case of PWA, pseudo-sinusoid maxima and minima fall in correspondence of the P wave; in case of QRSA, pseudo-sinusoid maxima and minima fall in correspondence of the QRS complex; and in case of TWA, pseudo-sinusoid maxima and minima fall in correspondence of the T wave.

if the input signal is the QRS signal, the pseudo-sinusoid signal is termed QRSA signal and has its maxima and minima in correspondence of the QRS complex; eventually, if the input signal is the T signal, the pseudo-sinusoid signal is termed TWA signal and has its maxima and minima in correspondence of the T wave. From each alternans signal, two features are extracted: the alternans amplitude (AAm; μV), defined as the difference between the maximum and the minimum of the alternans signal [40]; and the alternans area (AAr; μV × ms), defined as the product of AAm and the length of the analyzed wave (i.e. P-wave length, QRS-complex length and T-wave length, respectively).

2.3. Simulation study

The basic synthetic ECG tracing of the simulation study was obtained through a 64-fold repetition of a real heartbeat (i.e. NHB = 64) consisting of an electrocardiographic PQRST complex extracted from an ECG recording acquired on a healthy subject and not corrupted by noise or interference [44]. Each heartbeat was sampled at 200 Hz and was 750 ms long. Fundamental waves characterizing the considered heartbeat (P wave, R wave and T wave) had a monophasic positive polarity (amplitudes were: 0.24 mV, 2.76 mV and 0.77 mV, respectively). ECG sections used for alternans evaluation were located as follows: the P section ranged from 200 ms to 50 ms before the R peak and, thus, was 150 ms long; the QRS section ranged from 50 ms before to 50 ms after the R peak and, thus, was 100 ms long; eventually, the T section ranged from 50 ms to 320 ms after the R peak and, thus, was 270 ms long.

Stationary alternans affecting the synthetic ECG tracing was simulated by adding an alternating rectangular waveform to the different considered waves [45]. All possible combinations of alternans kinds were considered (Fig. 5).

Overall, 27 simulations (termed S1 to S27; Table 1) representing combinations of alternans kinds (PWA and/or QRSA and/or TWA) with low amplitude and high amplitude were evaluated. Low AAm values were quantified as 10 μV; consequently, corresponding AAr values relative to PWA, QRSA and TWA were equal to 1000 μV × ms, 800 μV × ms and 2000 μV × ms, respectively. High AAm values were quantified as 100 μV; consequently, corresponding AAr values relative to PWA, QRSA and TWA were equal to 10000 μV × ms, 8000 μV × ms and 20000 μV × ms, respectively. Heart rate was constant and equal to 80 bpm; consequently, f_A was equal to 0.67 Hz.

2.4. Experimental study

The experimental data consisted of standard 12-lead ECG recordings from 266 heart failure patients having an implanted cardioverter defibrillator (ICD) for primary prevention. Acquisitions were performed during a 10-min bicycle exercise test during which ECG recordings were acquired by a CASE 8000 stress test recorder (GE Healthcare, Freiburg, Germany; sampling frequency: 500 Hz; resolution: 4.88 μV/LSB); 3 M Red Dot ECG Electrode Soft Cloth 2271 electrodes were applied in accordance with the Mason-Likar configuration). All experimental data used in the present study belong to the Leiden University Medical Center ECG database [42]. According to "Guideline for Good Clinical Practice" (European Medicines Agency, CPMP/ICH/135/95) and the data privacy law in The Netherlands, no patients' informed consent was necessary since their data were anonymized and were recorded during routine medical care, without experimental interventions.

ECGA analysis was performed by recursively (NS = 2 s) extracting single lead ECG windows (NHB = 64). Each lead was analyzed independently. To be included in the analysis, the patient had to have at least one ECG window characterized by stable heart rate (i.e. stdRR<10 % mRR) and 9 leads with a number of replaced heartbeats less than 6 (i.e. lower than 10 % NHB), thus suitable for ECGA identification. For each enrolled patient, if more than one ECG window was suitable within an ECG recording, only the first one was considered.

2.5. Statistics

In the simulation study, EAMF performance in automatically identifying different kinds of alternans characterized by low and high amplitude was established by computation of the error (ε; %) defined in (2):

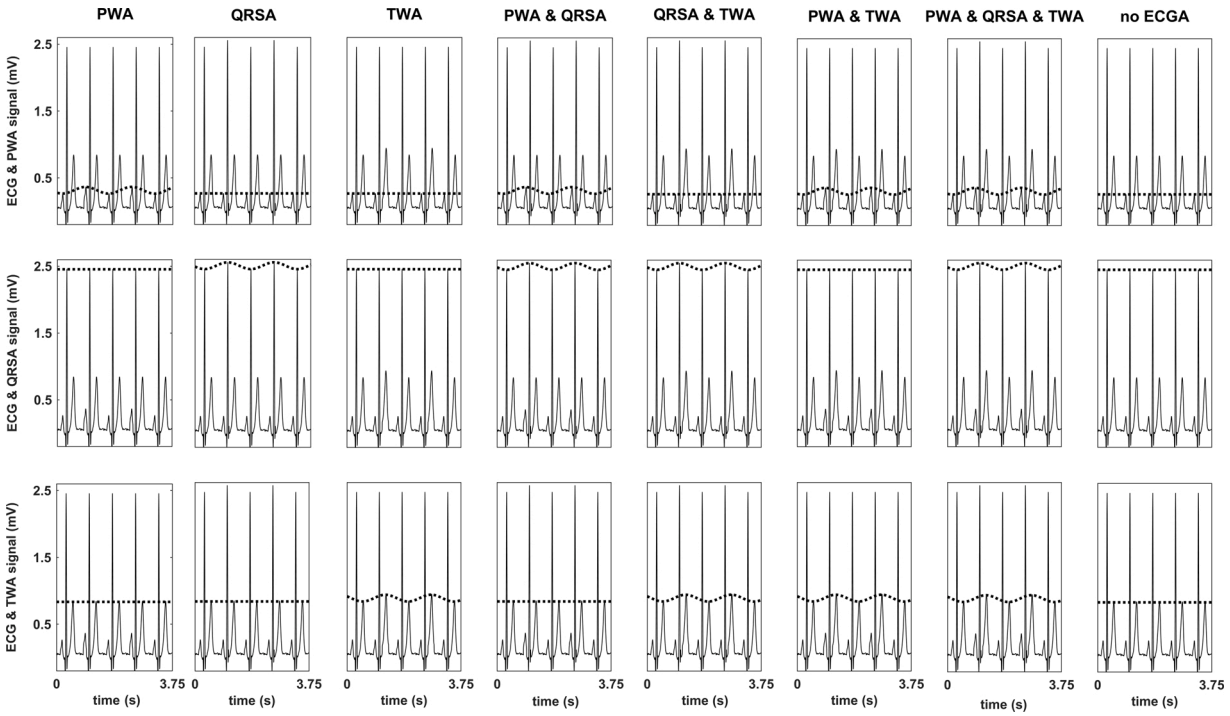

Fig. 5. Possible combinations of P-wave alternans (PWA), QRS-complex alternans (QRSA) and T-wave alternans (TWA) highlighted by plotting the alternans signals (dotted lines) over the electrocardiographic tracings (solid lines). Case of no electrocardiographic alternans (ECGA) is also depicted.

$$\varepsilon = \frac{Estimated\ AAm\ -\ Simulated\ AAm}{Simulated\ AAm} \cdot 100 = \frac{Estimated\ AAr\ -\ Simulated\ AAr}{Simulated\ AAr} \cdot 100 \quad (2)$$

Negative errors indicate alternans underestimations, while positive errors indicate overestimations. In (2), ε can been defined using either AAm or AAr, being AAr given by the product of AAm by wave length. Thus, ε quantifies both errors percent in AAm and AAr estimations.

In the experimental study, each lead previously found to be suitable for ECGA identification was characterized by six measures, that were AAm and AAr values for PWA, QRSA and TWA, respectively. The prevalent kind of alternans was defined as the one showing the highest AAr. AAm and AAr distribution over ICD patients or over leads were described in terms of median value and interquartile range (iqr). Comparisons were performed using the Wilcoxon signed rank test. Statistically significant level was set at 0.05 in all cases.

3. Results

3.1. Simulation study

The results of the simulation study are reported in Table 1 and in Table 2. Table 1 shows simulated and estimated values of AAm and AAr, while Table 2 shows alternans estimation errors.

Overall, EAMF accurately measured alternans in all simulated cases. Low amplitude alternans (AAm = 10 μV; S1 to S7, S15 to S26) was always perfectly estimated (ε = 0 %), independently by the alternating wave and by the number of waves simultaneously showing alternans. High amplitude alternans (AAm = 100 μV; S8 to S26) was slightly underestimated ($-2\ \% \leq \varepsilon \leq -1\ \%$). Underestimation was smaller in case of PWA ($|\varepsilon| = 1$ %) than in case of QRSA and TWA ($|\varepsilon| = 2$ %), independently by the number of waves simultaneously showing alternans. Eventually, absence of alternans was always correctly detected (ε = 0 %), either when characterizing one wave (S4 to S6, S11 to S13, S15 to S20), two waves (S1 to S3, S8 to S10) and all three waves (S27).

3.2. Experimental study

Overall, 187 ICD patients out of 266 (i.e. 70.3 % of the population) satisfied the inclusion criteria of the study and their ECG tracings were then processed for ECGA identification and measurement. The results of the experimental study are reported in Tables 3 and 4. Table 3 shows the prevalence rate of PWA, QRSA and TWA, together with rate of ECGA absence and rate of lead rejection; Table 4 shows AAm and AAr values (median (iqr)) characterizing identified PWA, QRSA and TWA. Complete absence of alternans was rarely present (rate of no ECGA over leads varied from 0 % to 4 %). In all cases in which alternans was present, it was found to be a lead-dependent phenomenon with the prevalent alternans always discriminable (i.e. there were no two or more waves characterized by the same AAr value). Independently by the lead, TWA was the prevalent alternans, always followed by QRSA and PWA. However, higher AAr values charactering TWA was mainly due to a higher T-wave length than to a higher AAm. Indeed, comparable clinical values of AAm (in all cases <10 μV, even though sometimes statistically different) were observed among alternans kinds in the same lead, and among leads for the same alternans kind. Rejection rate was very high on lead I (65 %) and aVL (40 %), moderate on lead aVR (13 %) and V5 (11 %), and small (<10 %) in all other leads.

Table 1
Results of the simulation study in terms of simulated and estimated AAm and AAr for all combinations of PWA, QRSA and TWA characterized by low (10 μV) and high (100 μV) amplitudes.

S	Simulated Alternans			Estimated Alternans		
	PWA AAm;AAr (μV;μV × ms)	QRSA AAm;AAr (μV;μV × ms)	TWA AAm;AAr (μV;μV × ms)	PWA AAm;AAr (μV;μV × ms)	QRSA AAm;AAr (μV;μV × ms)	TWA AAm;AAr (μV;μV × ms)
S1	10;1000	0;0	0;0	10;1000	0;0	0;0
S2	0;0	10;800	0;0	0;0	10;800	0;0
S3	0;0	0;0	10;2000	0;0	0;0	10;2000
S4	10;1000	10;800	0;0	10;1000	10;800	0;0
S5	0;0	10;800	10;2000	0;0	10;800	10;2000
S6	10;1000	0;0	10;2000	10;1000	0;0	10;2000
S7	10;1000	10;800	10;2000	10;1000	10;800	10;2000
S8	100;10000	0;0	0;0	99;9900	0;0	0;0
S9	0;0	100;8000	0;0	0;0	98;7840	0;0
S10	0;0	0;0	100;20000	0;0	0;0	98;19600
S11	100;10000	100;8000	0;0	99;9900	98;7840	0;0
S12	0;0	100;8000	100;20000	0;0	98;7840	98;19600
S13	100;10000	0;0	100;20000	99;9900	0;0	98;19600
S14	100;10000	100;8000	100;20000	99;9900	98;7840	98;19600
S15	10;1000	100;8000	0;0	10;1000	98;7840	0;0
S16	100;10000	10;800	0;0	99;9900	10;800	0;0
S17	10;1000	0;0	100;20000	10;1000	0;0	98;19600
S18	100;10000	0;0	10;2000	99;9900	0;0	10;2000
S19	0;0	10;800	100;20000	0;0	10;800	98;19600
S20	0;0	100;8000	10;2000	0;0	98;7840	10;2000
S21	10;1000	10;800	100;20000	10;1000	10;800	98;19600
S22	10;1000	100;8000	10;2000	10;1000	98;7840	10;2000
S23	100;10000	10;800	10;2000	99;9900	10;800	10;2000
S24	100;10000	100;8000	10;2000	99;9900	98;7840	10;2000
S25	100;10000	10;800	100;20000	99;9900	10;800	98;19600
S26	10;1000	100;8000	100;20000	10;1000	98;7840	98;19600
S27	0;0	0;0	0;0	0;0	0;0	0;0

AAm: Alternans Amplitude; AAr: Alternans Area; PWA: P-Wave Alternans; QRSA: QRS-complex Alternans; TWA: T-Wave Alternans.
S: Simulation.

Table 2
Results of the simulation study in terms of errors in alternans estimation for all combinations of PWA, QRSA and TWA characterized by low (10 μV) and high (100 μV) amplitudes.

S	PWA ε (%)	QRSA ε (%)	TWA ε (%)
S1	0	0	0
S2	0	0	0
S3	0	0	0
S4	0	0	0
S5	0	0	0
S6	0	0	0
S7	0	0	0
S8	−1	0	0
S9	0	−2	0
S10	0	0	−2
S11	−1	−2	0
S12	0	−2	−2
S13	−1	0	−2
S14	−1	−2	−2
S15	0	−2	0
S16	−1	0	0
S17	0	0	−2
S18	−1	0	0
S19	0	0	−2
S20	0	−2	0
S21	0	0	−2
S22	0	−2	0
S23	−1	0	0
S24	−1	−2	0
S25	−1	0	−2
S26	0	−2	−2
S27	0	0	0

PWA: P-Wave Alternans; QRSA: QRS-complex Alternans; TWA: T-Wave Alternans; S: Simulation; ε: error.

4. Discussion

The present study presents EAMF as the first reliable automated method to identify and measure ECGA in all its possible single or multiple manifestations as PWA, QRSA or TWA. EAMF represents an enhanced version of the heart-rate adaptive matched filter, previously proposed only for automated TWA measurement [40].

Analogously to the algorithm from which it derives, EAMF properly deals with ECG signals acquired in most clinical conditions. Indeed, it is based on a band-pass filter that tolerates physiological levels of heart-rate variability and filters out all the frequency components not pertaining to the alternans, such those related to noise [46]. Due to the theoretical approach on which it relies, EAMF is able to identify and measure ECGA independently of polarity of alternating waves. The filtering procedure does not alter the phase of the frequency component characterizing ECGA (and thus its time occurrence along the ECG) since the filter is implemented bidirectionally. Additionally, the possibility of setting the number of analyzed heartbeats (i.e. NHB) and the ECG-window extraction period (i.e. NS) allows EAMF application also to ECG tests with varying heart rate, since short ECG windows more likely respect the required heart-rate stability criterion and their frequent extraction allows a continuous adapting alternans analysis along the ECG. However, differently from the previously proposed heart-rate adaptive matched filter, EAMF is able to identify and measure PWA and QRSA in addition to TWA, and to discriminate which alternans kind among the three possible ones is the prevalent alternans. Technically, our methodological improvements mainly consist in the introduction of a signal enhancement procedure in the preprocessing step according to which all ECG sections but the one for which alternans has to be evaluated are set to baseline, and in the extraction of a new feature, the alternans area, in the alternans identification and measurement step. The signal enhancement procedure was introduced because the presence of different kinds of alternans simultaneously affecting the ECG may bias reliable alternans identification [39]. Indeed, the output of the band-pass filter is a pseudo-sinusoid signal the amplitude of which integrates all the possible alternans present in the ECG. In previous applications the occurrence of TWA was established by analyzing the pseudo-sinusoid phase, i.e. by checking that its maxima and minima would occur in correspondence of the T wave [40]. From a theoretical point of view, however, the maxima and the minima of the pseudo-sinusoid occur in correspondence of the center of mass of all ECG alternations [39]. Thus, for example, the simultaneous presence of both PWA and TWA could be erroneously measured as QRSA, since the alternans center of mass is in between the P wave and the T wave. The signal enhancement procedure solves this issue by deleting all waves but the one of interest and allows independent analysis of all alternans kinds. Additionally, it has been previously demonstrated that use of the band-pass filter for automated alternans measurement provides a value of alternans amplitude as if it was uniformly distributed over the alternating wave [47]. This means that the same alternans amplitude measured in waves of completely different lengths (such as the P wave

Table 3
Results of the experimental study in terms of rates, in percentage (%) of prevalent ECGA, ECGA absence and rejections.

ECG lead	PWA (%)	QRSA (%)	TWA (%)	No ECGA (%)	Rejection (%)
I	4	5	23	3	65
II	4	13	80	0	3
II	5	14	72	0	9
V1	3	17	69	2	9
V2	5	19	70	2	4
V3	3	14	75	2	6
V4	6	20	67	2	5
V5	4	19	65	1	11
V6	6	18	66	3	7
aVR	7	10	66	4	13
aVL	5	11	42	2	40
aVF	3	13	79	1	4

ECG: ElectroCardioGram; ECGA: ECG Alternans; PWA: P-Wave Alternans; QRSA: QRS-complex Alternans; TWA: T-Wave Alternans.

Table 4
Results of the experimental study in terms of estimated values characterizing PWA, QRSA and TWA.

ECG lead	ECGA features	PWA Median (iqr)	QRSA Median (iqr)	TWA Median (iqr)
I	AAm (μV)	4 (6)	6 (7)	5 (5)
	AAr (μV × ms)	426 (602)*	500 (548)*	902 (933)
II	AAm (μV)	8 (8)	11 (11)*	9 (7)
	AAr (μV × ms)	760 (763)*	890 (904)*	1725 (1390)
III	AAm (μV)	7 (7)	11 (12)*	9 (6)
	AAr (μV × ms)	728 (787)*	890 (1006)*	1706 (1367)
V1	AAm (μV)	4 (5)	9 (8)*	6 (6)
	AAr (μV × ms)	352 (498)*	693 (642)*	1124 (1199)
V2	AAm (μV)	4 (7)	10 (13)*	7 (8)
	AAr (μV × ms)	449 (624)*	828 (1086)*	1454 (1606)
V3	AAm (μV)	6 (7)	12 (13)*	8 (9)
	AAr (μV × ms)	575 (732)*	955 (1062)*	1629 (1814)
V4	AAm (μV)	5 (7)	10 (10)*	7 (6)
	AAr (μV × ms)	534 (679)*	826 (851)*	1496 (1320)
V5	AAm (μV)	5 (7)	11 (13)*	8 (8)
	AAr (μV × ms)	547 (651)*	891 (1042)*	1533 (1725)
V6	AAm (μV)	5 (6)	9 (9)*	6 (6)
	AAr (μV × ms)	501 (676)*	750 (791)*	1267 (1313)
aVR	AAm (μV)	5 (6)	7 (7)*	6 (5)
	AAr (μV × ms)	506 (602)*	547 (584)*	1136 (997)
aVL	AAm (μV)	5 (5)	8 (7)	5 (4)
	AAr (μV × ms)	500 (458)*	623 (566)*	1059 (930)
aVF	AAm (μV)	7 (7)	9 (12)*	8 (7)
	AAr (μV × ms)	665 (708)*	750 (980)*	1549 (1256)
Tot	AAm (μV)	5 (7)	9 (10)	7 (6)
	AAr (μV × ms)	545 (648)	762 (839)	1382 (1321)

AAm: Alternans Amplitude; AAr: Alternans Area; ECG: ElectroCardioGram; ECGA: ECG Alternans; PWA: P-Wave Alternans; QRSA: QRS-complex Alternans; TWA: T-Wave Alternans.

and the T wave) may involve a completely different amount of alternating ECG and, thus, possibly a completely different number of cardiac cells the action potential of which presents anomalies driving to alternans. Introduction of the alternans area as alternans feature in addition to alternans amplitude allows overcoming of this issue by providing information about the cumulative amount of alternans related to a specific wave. In order to simultaneously provide information relative to PWA, QRSA and TWA, EAMF had to introduce an ECG sectioning procedure to discriminate among the three waves. Being alternans related to the electrical activity of the cardiac cells, only the ECG portion between P-wave onset and T-wave end was considered (indeed, ECG baseline represents absence of electrical activity in the cardiac cells). The exact localization of ECG-section landmarks is not crucial here; indeed, for ECGA detection purpose, the only notable requirement is that each section must include the wave of interest. Therefore, a procedure of landmark localization based on experimental formulas might be also considered suitable.

EAMF ability to automatically identify, measure and discriminate all kinds of alternans was evaluated in both simulated and experimental conditions. The results of the simulation study demonstrate the ability of the EAMF to accurately identify all kinds of alternans (from that involving only one wave, to that involving two waves, till that involving all three waves; Table 1), independently on alternans amplitude and without providing false-positive detections. Indeed, estimation errors were at most 2 % in module in all cases (Table 2). These results were achieved thanks to the signal enhancement procedure. Indeed, preliminary results [39] obtained by application of the method without performing the signal enhancement procedure indicate that only alternans involving a single wave is correctly identified. Instead, significant errors occur when two or three waves are involved in the alternans. For example, in case both P wave and QRS complex are alternating of the same amount, only PWA would be identified (being P wave longer than QRS complex and thus AAr related to PWA greater than AAr related to QRSA) with significant errors (ε=+70 % for PWA and ε=−100 % for QRSA) indicating a strong overestimation of PWA, since QRSA is not recognized and wrongly associated to PWA. For all alternans combinations involving the T wave and characterized by the same amplitude, only TWA would be identified and strongly overestimated since T-wave length overcomes the sum of P-wave length and QRS-complex length. Eventually, if alternans involves two or more waves but with different amplitudes, only the wave in correspondence of which the center of mass occurs would be recognized as alternating and its alternans amplitude would be overestimated (the exact value depends on the alternans amplitudes combination).

In order to experimentally evaluate it, the EAMF was applied to ECG tracings acquired from ICD patients while performing physical activity. The goal was to demonstrate EAMF usability on real data, to investigate if different kinds of alternans could be simultaneously present and, in case of alternans affecting more than one wave, to evaluate if it is possible to discriminate the prevalent kind of alternans. The experimental results indicate that all three kinds of alternans may be simultaneously present, even if one is possibly dominant over the others. In particular, in our ICD patients all three kinds of alternans were always present even if TWA was the prevalent one, followed by QRSA and PWA (Table 3). These results are in agreement with the physiological observation that ICD patients are known to be at increased risk of major cardiac complications more often related to ventricles (the electrical activity of which is represented by the electrocardiographic QRS complex and T wave) than to atria (the electrical activity of which is represented by the ECG P wave) [48]. Moreover, this methodological study demonstrated how, in order to discriminate the prevalent alternans, it is necessary to consider the alternans area (i.e. AAr, here proposed for the first time) since it combines information related to both intensity and duration of the alternans phenomenon (represented by the alternans amplitude and wave length, respectively). Indeed, it might occur (as in our ICD patients) that mean alternans amplitude is comparable among ECG waves, and differentiation among alternans kinds is more evident in terms of alternating areas. Eventually, results of the experimental study confirmed that ECGA, in all its forms, is lead dependent, similarly to what observed for TWA [43].

It is finally important to reiterate that the present one represents a methodological study finalized to present and test the EAMF. Future clinical evaluations are needed to demonstrate the incremental clinical utility of ECGA as an index of cardiac risk with respect to TWA only.

5. Conclusion

In conclusion, the enhanced adaptive matched filter showed to be a reliable automated tool for accurately identify and measure electrocardiographic alternans in all its possible single or multiple manifestations as P-wave alternans, QRS-complex alternans or T-wave alternans. These unique achievements were obtained by improving the previously proposed heart-rate adaptive matched filter for T-wave alternans measurement. The improvements mainly consist in the introduction of a signal enhancement procedure in the preprocessing step, and in the extraction of the new feature termed alternans area, in the identification and measurement step. Availability of this tool will permit to simultaneously identify and measure P-wave alternans, QRS-complex alternans and T-wave alternans rather than only T-wave alternans (as usually done at the present time) and, possibly, to increment the prognostic value of electrocardiographic alternans.

Funding

This research did not receive any specific grant from funding agencies in the public, commercial, or not-for-profit sectors.

CRediT authorship contribution statement

Ilaria Marcantoni: Conceptualization, Methodology, Software, Writing - original draft. **Agnese Sbrollini:** Formal analysis, Writing - original draft. **Micaela Morettini:** Formal analysis, Writing - review & editing. **Cees A. Swenne:** Supervision, Writing - review & editing. **Laura Burattini:** Supervision, Project administration, Formal analysis, Writing - review & editing.

Declaration of Competing Interest

The authors declare that they have no known competing financial interests or personal relationships that could have appeared to influence the work reported in this paper.

References

[1] G. Tse, S.T. Wong, V. Tse, Y.T. Lee, H.Y. Lin, J.M. Yeo, Cardiac dynamics: alternans and arrhythmogenesis, J. Arrhythm. 32 (2016) 411–417, https://doi.org/10.1016/j.joa.2016.02.009.

[2] G. Kanaporis, L.A. Blatter, The mechanisms of calcium cycling and action potential dynamics in cardiac alternans, Circ. Res. 116 (2015) 846–856, https://doi.org/10.1161/CIRCRESAHA.116.305404.

[3] L. Burattini, W. Zareba, R. Burattini, Assessment of physiological amplitude, duration and magnitude of ECG T-wave alternans, Ann. Noninvasive Electrocardiol. 14 (2009) 366–374, https://doi.org/10.1111/j.1542-474X.2009.00326.x.

[4] R.L. Verrier, B.D. Nearing, M.T. La Rovere, G.D. Pinna, M.A. Mittleman, J. T. Bigger, P.J. Schwartz, ATRAMI Investigators, Ambulatory electrocardiogram-based tracking of T wave alternans in postmyocardial infarction patients to assess risk of cardiac arrest or arrhythmic death, J. Cardiovasc. Electrophysiol. 14 (2003) 705–711, https://doi.org/10.1046/j.1540-8167.2003.03118.x.

[5] R.L. Verrier, T. Nieminen, T-wave alternans as a therapeutic marker for antiarrhythmic agents, J. Cardiovasc. Pharmacol. 55 (2010) 544–554, https://doi.org/10.1097/FJC.0b013e3181d6b781.

[6] R.L. Verrier, T. Klingenheben, M. Malik, N. El-Sherif, D.V. Exner, S.H. Hohnloser, T. Ikeda, J.P. Martínez, S.M. Narayan, T. Nieminen, D.S. Rosenbaum, Microvolt T-wave alternans testing has a role in arrhythmia risk stratification, J. Am. Coll. Cardiol. 59 (2012) 1572–1573, https://doi.org/10.1016/j.jacc.2012.03.008.

[7] T. Nieminen, R.L. Verrier, Usefulness of T-wave alternans in sudden death risk stratification and guiding medical therapy, Ann. Noninvasive Electrocardiol. 15 (2010) 276–288, https://doi.org/10.1111/j.1542-474X.2010.00376.x.

[8] R.L. Verrier, T. Ikeda, Ambulatory ECG-based T-wave alternans monitoring for risk assessment and guiding medical therapy: mechanisms and clinical applications, Prog. Cardiovasc. Dis. 56 (2013) 172–185, https://doi.org/10.1016/j.pcad.2013.07.002.

[9] V. Shusterman, et al., Upsurge in T-wave alternans and nonalternating repolarization instability precedes spontaneous initiation of ventricular tachyarrhythmias in humans, Circulation 113 (2006) 2880–2887, https://doi.org/10.1161/CIRCULATIONAHA.105.607895.

[10] S.M. Narayan, T-wave alternans and the susceptibility to ventricular arrhythmias, J. Am. Coll. Cardiol. 47 (2006) 269–281, https://doi.org/10.1016/j.jacc.2005.08.066.

[11] D.M. Bloomfield, R.C. Steinman, P.B. Namerow, M. Parides, J. Davidenko, E. S. Kaufman, T. Shinn, A. Curtis, J. Fontaine, D. Holmes, A. Russo, C. Tang, J. T. Bigger, Microvolt T-wave alternans distinguishes between patients likely and patients not likely to benefit from implanted cardiac defibrillator therapy: a solution to the Multicenter Automatic Defibrillator Implantation Trial (MADIT) II conundrum, Circulation 110 (2004) 1885–1889, https://doi.org/10.1161/01.CIR.0000143160.14610.53.

[12] D.S. Rosenbaum, L.E. Jackson, J.M. Smith, H. Garan, J.N. Ruskin, R.J. Cohen, Electrical alternans and vulnerability to ventricular arrhythmias, N. Engl. J. Med. 330 (1994) 235–241, https://doi.org/10.1056/NEJM199401273300402.

[13] B. Vandenberk, V. Floré, C. Röver, M.A. Vos, A. Dunnink, D. Leftheriotis, T. Friede, P. Flevari, M. Zabel, R. Willems, Repeating noninvasive risk stratification improves prediction of outcome in ICD patients, Ann. Noninvasive Electrocardiol. 25 (2020), e12794, https://doi.org/10.1111/anec.12794.

[14] S. Kent, M. Ferguson, R. Trotta, L. Jordan, T wave alternans associated with HIV cardiomyopathy, erythromycin therapy, and electrolyte disturbances, South Med. J. 91 (1998) 755–758, https://doi.org/10.1097/00007611-199808000-00011.

[15] S.A. Siddiqi, J. Ulahannan, R. Storm, T-wave alternans in a hypothermic patient leading to unstable ventricular tachycardia, JACC Clin. Electrophysiol. 2 (2016) 640–641, https://doi.org/10.1016/j.jacep.2016.02.013.

[16] S. Figliozzi, A. Stazi, G. Pinnacchio, M. Laurito, R. Parrinello, A. Villano, G. Russo, M. Milo, R. Mollo, G.A. Lanza, F. Crea, Use of T-wave alternans in identifying patients with coronary artery disease, J. Cardiovasc. Med. 17 (2016) 20–25, https://doi.org/10.2459/JCM.0000000000000080.

[17] I. Donoiu, O.C. Mirea, A. Giuca, C. Militaru, D.D. Ionescu, Post-myocardial infarction arrhythmia risk stratification using microvolt T-wave alternans, Curr. Health Sci. J. 38 (2012) 65–68.

[18] T. Ikeda, H. Saito, K. Tanno, H. Shimizu, J. Watanabe, Y. Ohnishi, Y. Kasamaki, Y. Ozawa, T-wave alternans as a predictor for sudden cardiac death after myocardial infarction, Am. J. Cardiol. 89 (2002) 79–82, https://doi.org/10.1016/s0002-9149(01)02171-3.

[19] N. Takasugi, H. Goto, M. Takasugi, R.L. Verrier, T. Kuwahara, T. Kubota, H. Toyoshi, T. Nakashima, M. Kawasaki, K. Nishigaki, S. Minatoguchi, Prevalence of microvolt T-wave alternans in patients with long QT syndrome and its association with Torsade de Pointes, Circ. Arrhythm. Electrophysiol. 9 (2016), e003206, https://doi.org/10.1161/CIRCEP.115.003206.

[20] Y. Uchimura-Makita, Y. Nakano, T. Tokuyama, M. Fujiwara, Y. Watanabe, A. Sairaku, H. Kawazoe, H. Matsumura, N. Oda, H. Ikanaga, C. Motoda, K. Kajihara, N. Oda, R.L. Verrier, Y. Kihara, Time-domain T-wave alternans is strongly associated with a history of ventricular fibrillation in patients with Brugada syndrome, J. Cardiovasc. Electrophysiol. 25 (2014) 1021–1027, https://doi.org/10.1111/jce.12441.

[21] H. Shimada, M. Nishizaki, H. Fujii, N. Yamawake, S. Fukamizu, H. Sakurada, M. Hiraoka, Ambulatory electrocardiogram-based T-wave alternans in patients with vasospastic angina during asymptomatic periods, Am. J. Cardiol. 110 (2012) 1446–1451, https://doi.org/10.1016/j.amjcard.2012.06.054.

[22] R.L. Verrier, A.V. Tolat, M.E. Josephson, T-wave alternans for arrhythmia risk stratification in patients with idiopathic dilated cardiomyopathy, J. Am. Coll. Cardiol. 41 (2003) 2225–2227, https://doi.org/10.1016/s0735-1097(03)00466-2.

[23] E. Trzos, J.D. Kasprzak, M. Krzemińska-Pakuła, T. Rechciński, K. Wierzbowska-Drabik, B. Uznańska, A. Śmiałowski, T. Rudziński, M. Kurpesa, The prevalence and the prognostic value of microvolt T-wave alternans in patients with hypertrophic cardiomyopathy, Ann. Noninvasive Electrocardiol. 16 (2011) 276–286, https://doi.org/10.1111/j.1542-474X.2011.00443.x.

[24] R. Hojo, S. Fukamizu, T. Kitamura, K. Komiyama, Y. Tanabe, T. Tejima, M. Nishizaki, H. Sakurada, M. Hiraoka, Prominent J-wave and T-wave alternans associated with mechanical alternans in a patient with takotsubo cardiomyopathy, J. Arrhythm. 31 (2015) 43–46, https://doi.org/10.1016/j.joa.2014.03.008.

[25] S. Yamada, A. Yoshihisa, Y. Sato, T. Sato, M. Kamioka, T. Kaneshiro, M. Oikawa, A. Kobayashi, H. Suzuki, T. Ishida, Y. Takeishi, Utility of heart rate turbulence and T-wave alternans to assess risk for readmission and cardiac death in hospitalized heart failure patients, J. Cardiovasc. Electrophysiol. 29 (2018) 1257–1264, https://doi.org/10.1111/jce.13639.

[26] E. Siniorakis, S. Arvanitakis, P. Tzevelekos, N. Giannakopoulos, S. Limberi, P-wave alternans predicting imminent atrial flutter, Cardiol. J. 24 (2017) 706–707, https://doi.org/10.5603/CJ.2017.0147.

[27] G. Tsiaousis, N. Fragakis, P-wave alternans in a patient with hyponatremia, Hellenic J. Cardiol. 57 (2016) 188–190, https://doi.org/10.1016/j.hjc.2015.12.001.

[28] B. Brembilla-Perrot, H. Lucron, F. Schwalm, A. Haouzi, Mechanism of QRS electrical alternans, Heart 77 (1997) 180–182, https://doi.org/10.1136/hrt.77.2.180.

[29] R.L. Rinkenberger, R.A. Polumbo, M.R. Bolton, M. Dunn, Mechanism of electrical alternans in patients with pericardial effusion, Cathet. Cardiovasc. Diagn. 4 (1978) 63–70, https://doi.org/10.1002/ccd.1810040109.

[30] É.P. McCarron, M. Monaghan, S. Sreenivasan, Images of the month 2: electrocardiographic QRS alternans caused by gastric volvulus, Clin. Med. (Lond.) 19 (2019) 528–529, https://doi.org/10.7861/clinmed.2019-0259.

[31] P. Maury, J. Metzger, Alternans in QRS amplitude during ventricular tachycardia, Pacing Clin. Electrophysiol. 25 (2002) 142–150, https://doi.org/10.1046/j.1460-9592.2002.00142.x.

[32] G. Pulignano, N. Patruno, P. Urbani, C. Greco, G. Critelli, Electrophysiological significance of QRS alternans in narrow QRS tachycardia, Pacing Clin. Electrophysiol. 13 (1990) 144–150, https://doi.org/10.1111/j.1540-8159.1990.tb05063.x.

[33] N. Otsuka, K. Nagashima, Y. Wakamatsu, Y. Okumura, Supraventricular tachycardia with QRS alternans: what is the mechanism? J. Cardiovasc. Electrophysiol. 31 (2020) 1560–1562, https://doi.org/10.1111/jce.14508.

[34] K. Nakasuka, T. Noda, K. Miyamoto, K. Kusano, QRS alternans due to localized intraventricular block during ventricular tachycardia in Uhl's anomaly: a case report, Eur. Heart J. Case Rep. 3 (2019), ytz006, https://doi.org/10.1093/ehjcr/ytz006.

[35] D. Varvarousis, K. Polytarchou, P. Margos, S.N. Psychari, K. Paravolidakis, D. Tsoukalas, A. Kotsakis, Supraventricular tachycardia with QRS and cycle length alternans. What is the diagnosis? Hellenic J. Cardiol. 60 (2019) 331–333, https://doi.org/10.1016/j.hjc.2019.01.006.

[36] A. Suszko, S. Nayyar, C. Labos, K. Nanthakumar, A. Pinter, E. Crystal, V. S. Chauhan, Microvolt QRS alternans without microvolt T-wave alternans in human cardiomyopathy: a novel risk marker of late ventricular arrhythmias, J. Am. Heart Assoc. 9 (2020), e016461, https://doi.org/10.1161/JAHA.119.016461.

[37] S. Alaei, S. Wang, P. Anaya, A. Patwardhan, Co-occurrence and phase relationship between alternans of the R wave amplitude (RWAA) and of the T wave (TWA) in ECGs, Comput. Biol. Med. 121 (2020), 103785, https://doi.org/10.1016/j.compbiomed.2020.103785.

[38] K. Kulkarni, F.M. Merchant, M.B. Kassab, F. Sana, K. Moazzami, O. Sayadi, J. P. Singh, E.K. Heist, A.A. Armoundas, Cardiac alternans: mechanisms and clinical utility in arrhythmia prevention, J. Am. Heart Assoc. 8 (2019), e013750, https://doi.org/10.1161/JAHA.119.013750.

[39] I. Marcantoni, D. Calabrese, G. Chiriatti, R. Melchionda, B. Pambianco, G. Rafaiani, E. Scardecchia, A. Sbrollini, M. Morettini, L. Burattini, Electrocardiographic alternans: a new approach, in: MEDICON 2019, IFMBE Proc., Coimbra, PT, 2019, pp. 1–8, https://doi.org/10.1007/978-3-030-31635-8_19.

[40] L. Burattini, W. Zareba, R. Burattini, Adaptive match filter based method for time vs. amplitude characterization of microvolt ECG T-wave alternans, Ann. Biomed. Eng. 36 (2008) 1558–1564, https://doi.org/10.1007/s10439-008-9528-6.

[41] L. Burattini, W. Zareba, R. Burattini, Identification of gender-related normality regions for T-wave alternans, Ann. Noninvasive Electrocardiol. 15 (2010) 328–336, https://doi.org/10.1111/j.1542-474X.2010.00388.x.

[42] L. Burattini, S. Man, S. Fioretti, F. Di Nardo, C.A. Swenne, Heart rate-dependent hysteresis of T-wave alternans in primary prevention ICD patients, Ann. Noninvasive Electrocardiol. 21 (2016) 460–469, https://doi.org/10.1111/anec.12330.

[43] L. Burattini, S. Man, R. Burattini, C.A. Swenne, Comparison of standard versus orthogonal ECG leads for T-wave alternans identification, Ann. Noninvasive Electrocardiol. 17 (2012) 130–140, https://doi.org/10.1111/j.1542-474X.2012.00490.x.

[44] L. Burattini, S. Bini, R. Burattini, Repolarization alternans heterogeneity in healthy subjects and acute myocardial infarction patients, Med. Eng. Phys. 34 (2012) 305–312, https://doi.org/10.1016/j.medengphy.2011.07.019.

[45] L. Burattini, S. Bini, R. Burattini, Comparative analysis of methods for automatic detection and quantification of microvolt T-wave alternans, Med. Eng. Phys. 31 (2009) 1290–1298, https://doi.org/10.1016/j.medengphy.2009.08.009.

[46] L. Burattini, S. Bini, R. Burattini, Automatic microvolt T-wave alternans identification in relation to ECG interferences surviving preprocessing, Med. Eng. Phys. 33 (2011) 17–30, https://doi.org/10.1016/j.medengphy.2010.08.014.

[47] S. Bini, L. Burattini, Quantitative characterization of repolarization alternans in terms of amplitude and location: what information from different methods? Biomed. Signal Process. Control 8 (2013) 675–681, https://doi.org/10.1016/j.bspc.2013.06.012.

[48] S.C. Man, P.V. De Winter, A.C. Maan, J. Thijssen, C.J.W. Borleffs, W.P.M. van Meerwijk, M. Bootsma, L. van Erven, E.E. van der Wall, M.J. Schalij, L. Burattini, R. Burattini, C.A. Swenne, Predictive power of T-wave alternans and of ventricular gradient hysteresis for the occurrence of ventricular arrhythmias in primary prevention cardioverter-defibrillator patients, J. Electrocardiol. 44 (2011) 453–459, https://doi.org/10.1016/j.jelectrocard.2011.05.004.